

AFRL-VA-WP-TP-2006-307

**NONLINEAR FEEDBACK CONTROL
FOR RAPID, ON-LINE
TRAJECTORY OPTIMIZATION OF
REENTRY VEHICLES (PREPRINT)**

**Dr. David B. Doman
Kevin P. Bollino
I. Michael Ross**



DECEMBER 2005

Approved for public release; distribution is unlimited.

STINFO FINAL REPORT

This work has been submitted to AIAA for publication in the AIAA Atmospheric Flight Mechanics Conference proceedings. If this work is published, it is considered a work of the U.S. Government and is not subject to copyright in the United States.

**AIR VEHICLES DIRECTORATE
AIR FORCE RESEARCH LABORATORY
AIR FORCE MATERIEL COMMAND
WRIGHT-PATTERSON AIR FORCE BASE, OH 45433-7542**

NOTICE

Using Government drawings, specifications, or other data included in this document for any purpose other than Government procurement does not in any way obligate the U.S. Government. The fact that the Government formulated or supplied the drawings, specifications, or other data does not license the holder or any other person or corporation; or convey any rights or permission to manufacture, use, or sell any patented invention that may relate to them.

This report was cleared for public release by the Air Force Research Laboratory Wright Site (AFRL/WS) Public Affairs Office (PAO) and is releasable to the National Technical Information Service (NTIS). It will be available to the general public, including foreign nationals.

PAO Case Number: AFRL/WS-06-0083, 9 Jan 2006.

THIS TECHNICAL REPORT IS APPROVED FOR PUBLICATION.

/s/

David Doman
Senior Aerospace Engineer
Control Design and Analysis Branch
Air Force Research Laboratory
Air Vehicles Directorate

/s /

Deborah S. Grismer
Chief
Control Design and Analysis Branch
Air Force Research Laboratory
Air Vehicles Directorate

/s/

Brian W. Van Vliet
Chief
Control Sciences Division
Air Force Research Laboratory
Air Vehicles Directorate

This report is published in the interest of scientific and technical information exchange and its publication does not constitute the Government's approval or disapproval of its ideas or findings.

REPORT DOCUMENTATION PAGE					Form Approved OMB No. 0704-0188	
<p>The public reporting burden for this collection of information is estimated to average 1 hour per response, including the time for reviewing instructions, searching existing data sources, gathering and maintaining the data needed, and completing and reviewing the collection of information. Send comments regarding this burden estimate or any other aspect of this collection of information, including suggestions for reducing this burden, to Department of Defense, Washington Headquarters Services, Directorate for Information Operations and Reports (0704-0188), 1215 Jefferson Davis Highway, Suite 1204, Arlington, VA 22202-4302. Respondents should be aware that notwithstanding any other provision of law, no person shall be subject to any penalty for failing to comply with a collection of information if it does not display a currently valid OMB control number. PLEASE DO NOT RETURN YOUR FORM TO THE ABOVE ADDRESS.</p>						
1. REPORT DATE (DD-MM-YY) December 2005		2. REPORT TYPE Conference Paper Preprint		3. DATES COVERED (From - To) 12/19/2004 – 12/19/2005		
4. TITLE AND SUBTITLE NONLINEAR FEEDBACK CONTROL FOR RAPID, ON-LINE TRAJECTORY OPTIMIZATION OF REENTRY VEHICLES (PREPRINT)				5a. CONTRACT NUMBER In-house		
				5b. GRANT NUMBER		
				5c. PROGRAM ELEMENT NUMBER N/A		
6. AUTHOR(S) David B. Doman (AFRL/VACA) Kevin P. Bollino and I. Michael Ross (Naval Postgraduate School)				5d. PROJECT NUMBER N/A		
				5e. TASK NUMBER N/A		
				5f. WORK UNIT NUMBER N/A		
7. PERFORMING ORGANIZATION NAME(S) AND ADDRESS(ES) Control Design and Analysis Branch (AFRL/VACA) Control Sciences Division Air Vehicles Directorate Air Force Research Laboratory, Air Force Materiel Command Wright-Patterson AFB, OH 45433-7542				8. PERFORMING ORGANIZATION REPORT NUMBER AFRL-VA-WP-TP-2006-307		
9. SPONSORING/MONITORING AGENCY NAME(S) AND ADDRESS(ES) Air Vehicles Directorate Air Force Research Laboratory Air Force Materiel Command Wright-Patterson Air Force Base, OH 45433-7542				10. SPONSORING/MONITORING AGENCY ACRONYM(S) AFRL/VACA		
				11. SPONSORING/MONITORING AGENCY REPORT NUMBER(S) AFRL-VA-WP-TP-2006-307		
12. DISTRIBUTION/AVAILABILITY STATEMENT Approved for public release; distribution is unlimited.						
13. SUPPLEMENTARY NOTES Conference paper preprint to be presented at the AIAA Atmospheric Flight Mechanics Conference, 24 Aug 06, Keystone, CO. This work has been submitted to AIAA for publication in the AIAA Atmospheric Flight Mechanics Conference proceedings. If this work is published, it is considered a work of the U.S. Government and is not subject to copyright in the United States.						
14. ABSTRACT A new, on-line sampled-data feedback control algorithm for fast and accurate nonlinear optimal closed-loop control of a generic reentry vehicle in the presence of disturbances is presented. A direct Legendre pseudospectral method is used for the rapid re-computation of the open-loop optimal controls such that a successive optimal solution is fed back to the system to help manage uncertainties and external disturbances. The method is based on a receding-horizon control approach, but does not require and advanced knowledge of the computation time. Successful performance of this approach, combined with a spectral algorithm, shows that rapid trajectory generation is not only achievable, but that it is fast enough to provide optimal closed-loop feedback with successive re-computations.						
15. SUBJECT TERMS						
16. SECURITY CLASSIFICATION OF:			17. LIMITATION OF ABSTRACT: SAR	18. NUMBER OF PAGES 28	19a. NAME OF RESPONSIBLE PERSON (Monitor) Dr. David B. Doman 19b. TELEPHONE NUMBER (Include Area Code) (937) 255-8451	
a. REPORT Unclassified	b. ABSTRACT Unclassified	c. THIS PAGE Unclassified				

Nonlinear Feedback Control for Rapid, On-line Trajectory Optimization of Reentry Vehicles*

Kevin P. Bollino[†] and I. Michael Ross[‡]

Naval Postgraduate School, Monterey, CA 93940

David D. Doman^{‡‡}

Air Force Research Laboratory, WPAFB, OH 45433-7531

Abstract

Rapid, on-line trajectory generation for reusable launch vehicles is gaining high interest with the explosive desire for more intelligent and autonomous systems. There are many aspects that make such achievement very appealing, such as being able to autonomously re-plan a mission on-the-fly in the case of abort guidance. Due to the constrained, highly nonlinear nature of the reentry problem, feasible and computationally-efficient guidance and control methods have been a challenge since the beginning of the space age. This paper demonstrates the feasibility of using a new, on-line sampled-data feedback control algorithm for fast and accurate nonlinear optimal closed-loop control of a generic reentry vehicle in the presence of disturbances. A direct Legendre pseudospectral method is used for the rapid re-computation of the open-loop optimal controls such that a successive optimal solution is fed back to the system to help manage uncertainties and external disturbances. The method is based on a receding-horizon control approach, but does not require any prior knowledge of the computation time. Successful performance of this approach, combined with a spectral algorithm, shows that rapid trajectory generation is not only achievable, but that it is fast enough to provide optimal closed-loop feedback with successive re-computations.

*This material is declared a work of the U.S. Government and is not subject to copyright protection in the United States.

[†]Ph.D. Candidate, Department of Mechanical and Astronautical Engineering, Guidance, Navigation, and Control Lab, Ph. 831-656-3183, Email: kpbollin@nps.edu, AIAA Member.

[‡]Professor, Department of Mechanical and Astronautical Engineering, Ph. 937-656-2074, Email: imross@nps.edu, AIAA Associate Fellow.

^{‡‡}Senior Aerospace Engineer, 2210 Eighth Street, Bldg. 146, Rm. 305, Ph. 937-255-8451, Email: David.Doman@wpafb.af.mil, Senior AIAA Member

1. Introduction

With ongoing efforts to improve the safety, reliability, and cost of reusable launch vehicle (RLV) systems and operations along with the more recent focus on a U.S Space Shuttle replacement following its retirement around 2012, there is a new opportunity to implement advanced, yet simpler and more effective guidance and control methods than used in previous launch technologies. A key objective that is sought in this endeavor as well as almost all other sectors of technology is the requirement for more intelligent systems that can operate autonomously without as much human interaction. Of course this has the underlying stipulation that they operate safer, more reliable, and more efficiently than before. To accomplish this objective for the case of a RLV, the guidance and control during ascent, reentry, or landing needs to autonomously happen on-line and in real-time. The RLV intelligent control (i.e. “brains”) needs to be capable of adapting to rapidly changing circumstances, handle large external disturbances, large parameter uncertainties, re-generate trajectories (i.e. re-plan how to get to a designated or alternate landing site), reconfigure its controls in the advent of an unforeseen control failure and then of course to figure out how to allocate the controls.

Originally, the challenge of solving constrained, highly nonlinear dynamics and the limitations of computational speed at the time, demanded linearized, approximate equations. Often, the control equations were driven with tediously derived gain-scheduled schemes such as the drag-based tracking techniques used in Space Shuttle entry guidance where a series of drag reference segments required individual controller gain design [1].

With the realization of advances in computational power and numerical algorithms, recent research efforts for solving the reentry problem have focused on real-time, on-line trajectory generation, guidance adaptation, and control reconfiguration. Oppenheimer, Bolender, and Doman at the Air Force Research Lab’s office of Advanced Guidance and Control have done extensive work on reconfigurable control in the form of an optimal control allocation algorithm for such vehicles as the X-40, X-37, and X-33 [2]-[4]. Reconfiguration capabilities for RLV guidance and control systems has also been rigorously pursued by others mainly in support of two program initiatives to support such work: Marshall Space Flight Center’s (MSFC) Advanced Guidance and Control (AG&C) Program and the Air Force Research Lab’s (AFRL) Integrated Adaptive Guidance and Control (IAG&C) Program. More on these programs can be found in Ref. [5] and [6].

Since control reconfiguration and guidance adaptation will not always be enough to recover a vehicle after control failures, Schierman et al, has taken this one step further by developing an architecture that allows for reshaping of the outer-loop guidance trajectory commands and retargeting an alternate landing site should the nominal or original mission be aborted [6,7]. Likewise, Shaffer has integrated this need of trajectory reshaping and retargeting with the reconfigurable control work of Oppenheimer et al., to demonstrate relatively fast computations of optimal trajectories under trim deficient path-constraints [8].

Moving away from the successful, but extremely time-consuming gain-scheduling approach for flight-control designs, numerous efforts have employed a form of feedback linearization, often referred to as dynamic inversion. Through the use of nonlinear feedback, dynamic inversion essentially cancels the nonlinearities of the system to form an augmented linear system that can

then be controlled using more traditional linear control techniques. Unfortunately, this linearization technique requires exact knowledge of the system model, such as specific plant parameters. For air vehicles where large uncertainties such as aerodynamics forces and moments are inevitable, this method could easily result in unstable, unrecoverable flight conditions. For this reason, other nonlinear feedback methods are being investigated. Some methods include various combinations of adaptive control, backstepping, and even more robust versions of dynamic inversion.

One way to address the problem is by using an optimal trajectory generator to solve for a reference input trajectory off-line, and then use other inner-loop control means to track the desired trajectory. Schierman et al. has recently demonstrated the use of an outer-loop optimal control scheme to generate a reference trajectory that is tracked by an LQR inner-loop controller [9]. In a similar fashion, Carson uses an outer-loop guidance scheme with LQR inner-loop feedback to manage disturbances and uncertainty [10]. Carson's work employs a method presented by Milam [11], whereby real-time trajectory generation is made possible by finding the trajectory curves in a lower dimensional space, parameterizing the curves with B-splines, and then using Sequential Quadratic Programming (SQP) to find the spline coefficients that satisfy the optimization objectives and constraints.

With online approaches becoming more capable of solving highly nonlinear systems, there is really no need for off-line designs of closed-loop feedback laws. In this paper, an intelligent trajectory guidance system is designed for a generic reentry vehicle by solving the optimal control problem online without an inner-loop tracking controller. Once provided the initial and final conditions for the reentry vehicle, the proposed algorithm computes the nonlinear optimal control. As in most control designs, feedback is required to manage uncertainties. For the reentry problem, parameter uncertainty and external disturbances such as wind gusts (or shear) cause the vehicle to deviate from its nominal trajectory that may have been the originally predicted/computed/planned optimal trajectory. The proposed guidance and control method, adapted from the promising work of Pooya, Fleming, and Ross on a spacecraft optimal-time slew maneuver [12], uses a sampled-data feedback law to provide an optimal trajectory in the presence of uncertainty and disturbances. Rather than track a pre-computed solution, the scheme re-solves the optimal control problem and updates the control command as soon as a new solution is calculated. This method is also similar to Schierman's Optimal-Path-to-Go (OPTG) Trajectory Reshaping Strategy presented in his early 2001 work [13]. The work presented herein differs from Schierman's in that it is primarily used for feedback without using an inner-loop tracking controller. The original concept dates back to the early 1990's, when Pesch discussed off-line and on-line methods for aerospace applications [14]. He introduced the combination of what he called the "Neighboring Optimal Feedback Guidance" with a "Repeated Correction Guidance Scheme" to essentially perform the same objective as the method presented in Pooya's work [12]. The main difference is that his method relied on a linearized indirect multiple shooting technique that requires a more complicated implementation at increased computational cost. Unlike Pesch's "repeated correction method," the method presented in this paper guarantees that the constraints are satisfied before feeding back the control signal provided there is a feasible solution. Also, it was claimed that the "theoretical and numerical basis" for the on-line approach is not mature enough for general optimal control problems. Although this paper

does not provide the “mathematical justification” that Pesch desires, it is yet another stepping-stone to making on-line trajectory optimization more practical.

To solve the optimal control problem, a spectral algorithm [15-18] known as the Legendre Pseudospectral Method is employed by use of a MATLAB-based software package called DIDO [19]. This direct method discretizes the problem and approximates the states, co-states and control variables by use of Lagrange interpolating polynomials where the unknown coefficient values coincide with the Legendre-Gauss-Lobatto (LGL) node points. After this approximation step, an NLP solver (SNOPT) solves a sequence of finite-dimensional optimization problems that capture the nonlinearities of the system in the form of an optimal control. For an extensive description of this method and its use for real-time optimal control, see references [15]-[21].

With a lot of interest in real-time trajectory generation, this paper intends to demonstrate that by using a fast psuedospectral optimization method, not only are rapid optimal trajectories achievable, but through successive trajectory generations as a nonlinear sampled-data feedback law, optimal guidance and control is attained in the presence of parameter uncertainty and external disturbances.

2. Problem Definition & Formulation

2.1 Reentry Model (Kinematics and Dynamics)

Using a reduced-order model is all that is required to clearly demonstrate that the nonlinear feedback technique is an effective method towards reentry trajectory optimization. Therefore, for this paper, the full 6-DOF equations of motion are simplified and decoupled to create a reduced-order model. The model assumes a point-mass-model over a flat, non-rotating earth such that the positional and translational equations of motion in a Cartesian “local horizontal” coordinate system become

$$\begin{aligned}
 \dot{x} &= V \cos \mathbf{g} \cos \mathbf{x} \\
 \dot{y} &= V \cos \mathbf{g} \sin \mathbf{x} \\
 \dot{z} &= V \sin \mathbf{g} \\
 \dot{V} &= -\frac{D\{V, z\}}{m} - g \sin \mathbf{g} \\
 \dot{\mathbf{g}} &= \frac{L\{V, z\}}{mV} - \frac{g \cos \mathbf{g}}{V} \\
 \dot{\mathbf{x}} &= \frac{L\{V, z\} \sin \mathbf{s}}{mV \cos \mathbf{g}}
 \end{aligned} \tag{1}$$

Where x (down-range), y (cross-range), and z (altitude) are the vehicle’s position with respect to the fixed-earth reference frame, V is the velocity magnitude (i.e. total airspeed), \mathbf{g} is the flight-path-angle (FPA), \mathbf{x} is the heading angle, \mathbf{a} is the angle-of-attack (AoA), and \mathbf{s} is the angle-of-bank (AoB).

The lift and drag forces are represented as L and D , respectively, given by

$$L = \frac{1}{2} \mathbf{r}\{z\} V^2 C_L \{\mathbf{a}\} S_{ref} = \frac{1}{2} (\mathbf{r}_0 e^{-z/z_0}) V^2 C_L \{\mathbf{a}\} S_{ref} \quad (2)$$

$$D = \frac{1}{2} \mathbf{r}\{z\} V^2 C_D \{\mathbf{a}\} S_{ref} = \frac{1}{2} (\mathbf{r}_0 e^{-z/z_0}) V^2 C_D \{\mathbf{a}\} S_{ref} \quad (3)$$

where S_{ref} is the reference area given as 1600 ft², the term $\frac{1}{2} \mathbf{r}(z) V^2$ is the dynamic pressure, \bar{q} , and the term $\mathbf{r}_0 e^{-z/z_0}$ is the commonly accepted two-parameter model for atmospheric density, \mathbf{r} , as a function of altitude. This density approximation, where ρ_0 is the reference density taken to be 1.725 kg/m³ (0.003399 slugs/ft³), z is the current altitude, and z_0 is the atmospheric scale height (i.e. reference height) taken to be 6700 m (21981.6 ft), is good for closed-form solutions and fits well from 5 to 40 km in altitude [22].

For simplicity, the coefficients of lift (C_L) and drag (C_D) are modeled as

$$C_L \{\mathbf{a}\} = C_{L_0} + C_{L_a} \mathbf{a} \quad (4)$$

$$C_D \{\mathbf{a}\} = C_{D_0} + C_{D_a} \mathbf{a} + C_{D_{a^2}} \mathbf{a}^2 \quad (5)$$

Where the coefficients are

$C_{L_0} = -0.2070$, $C_{L_a} = 0.0292$, $C_{D_0} = 0.0785$, $C_{D_a} = -0.6159 \times 10^{-2}$, and $C_{D_{a^2}} = 0.6214 \times 10^{-3}$ with \mathbf{a} in degrees [23].

To fully capture the state at any instant, the state vector for this reduced-order model is given as

$$\underline{x} = [x \ y \ z \ V \ \mathbf{g} \ \mathbf{x}]^T \in \mathbb{R}^6 \quad (6)$$

Without a thrust force for the reentry gliding problem, the only controllable parameters for this reduced-order model are the lift and drag forces. Typically, for symmetric flight (i.e. coordinated turns where $\mathbf{b} = 0$), the lift and drag coefficients can be determined by the vehicle's angle-of-attack and Mach number, a function of velocity and speed-of-sound at a given altitude. However, it is the physical modulation of angle-of-attack and bank angle that controls the vehicle's translational motion through x-y-z space. Therefore, a common control vector for the reentry problem is

$$\underline{u} = [\mathbf{a} \ \mathbf{s}]^T \in \mathbb{R}^2 \quad (7)$$

Of course with these control variables defining the control vector, it is assumed that there are no command delays (i.e. lags), hence; this type of control is sometimes referred to as “inertialess” control. To help compensate for this and add a little realism to the problem, as explained in references [8] and [23], a new control vector is formed such that rate limits can be modeled as well. This is accomplished by using “virtual” controls [23] mathematically expressed as

$$\underline{u} = [u_a \ u_s]^T \in \mathbb{R}^2 \quad (8)$$

Now, since the algorithm uses these, the original state vector must include the physical controls, \mathbf{a} and \mathbf{s} , to form a new state vector:

$$\underline{x} = [x \ y \ z \ V \ \mathbf{g} \ \mathbf{x} \ \mathbf{a} \ \mathbf{s}]^T \in \mathbb{R}^8 \quad (9)$$

Remark: For a real vehicle, or in a 6-DOF simulation, it is the control surface deflections that create body moments and forces to augment the wind-relative angle-of-attack, bank angle, and sideslip angle.

2.2 General Problem Formulation

As with any dynamical optimization problem, the cost function (a.k.a objective function), governing equations of motions, path constraints, boundary limits on initial/final conditions, and any constraints (on states and/or controls) must be defined. As such, the general optimal control problem for trajectory generation is fully posed in the following manner:

$$\begin{aligned} \min_u J(\underline{x}(\mathbf{t}), \underline{u}(\mathbf{t}), \mathbf{t}_0, \mathbf{t}_f) &= E(\underline{x}(\mathbf{t}_0), \underline{x}(\mathbf{t}_f), \mathbf{t}_0, \mathbf{t}_f) + \int_{\mathbf{t}_0}^{\mathbf{t}_f} F(\underline{x}(\mathbf{t}), \underline{u}(\mathbf{t}), \mathbf{t}) d\mathbf{t} \\ \text{subject to} \quad \dot{\underline{x}} &= \underline{f}(\underline{x}, \underline{u}, \mathbf{t}) \\ \underline{h}_l &\leq \underline{h}(\underline{x}, \underline{u}, \mathbf{t}) \leq \underline{h}_u \\ \underline{e}_l &\leq \underline{e}(\underline{x}(\mathbf{t}_0), \underline{x}(\mathbf{t}_f), \mathbf{t}_0, \mathbf{t}_f) \leq \underline{e}_u \\ \underline{x}_l &\leq \underline{x}(\mathbf{t}) \leq \underline{x}_u \\ \underline{u}_l &\leq \underline{u}(\mathbf{t}) \leq \underline{u}_u \end{aligned} \quad (10)$$

The goal is to find a state-control function pair, $\{x(\cdot), u(\cdot)\}$, or sometimes time, \mathbf{t} , that minimizes the performance index represented by the Bolza form, $J(\cdot)$, consisting of either a Mayer term, $E(\cdot)$, a Lagrange term, $F(\cdot)$, or both as stated above.

2.3 Reentry Optimal Control Formulation

Summarizing the previous reentry equations, the specific optimal control formulation for this RV problem is stated as follows: Given an initial position vector $([x_0, y_0, z_0])$, velocity magnitude (V_0) , FPA (\mathbf{g}_0) , heading angle (\mathbf{x}_0) , AoA (\mathbf{a}_0) , and AoB (\mathbf{s}_0) , find the control history (u_a, u_s) that maximizes the horizontal downrange distance (x_f) under various constraints.

$$\mathbf{x}^T = [x, y, z, V, \mathbf{g}, \mathbf{x}, \mathbf{a}, \mathbf{s}] \quad \mathbf{u} = [u_a, u_s] \quad U = \{u_a, u_s \in \mathbb{R}^1 : -40 \frac{\text{deg}}{s} \leq u_a, u_s \leq 40 \frac{\text{deg}}{s}\}$$

$$\text{Min} \quad J[\mathbf{x}(t), \mathbf{u}(t), t_0, t_f] = -x_f$$

s.t.

$$\dot{x} = V \cos \mathbf{g} \cos \mathbf{x}$$

$$\dot{y} = V \cos \mathbf{g} \sin \mathbf{x}$$

$$\dot{z} = V \sin \mathbf{g}$$

$$\dot{V} = -\frac{D\{V, z\}}{m} - g \sin \mathbf{g}$$

$$\dot{\mathbf{g}} = \frac{L\{V, z\}}{m V} - \frac{g \cos \mathbf{g}}{V}$$

$$\dot{\mathbf{x}} = \frac{L\{V, z\} \sin \mathbf{s}}{m V \cos \mathbf{g}}$$

$$\dot{\mathbf{a}} = u_a,$$

$$\dot{\mathbf{s}} = u_s$$

$$(t_0, x_0, y_0, z_0, V_0, \mathbf{g}_0, \mathbf{x}_0, \mathbf{a}_0, \mathbf{s}_0) = (0, 0, 0, 125000\text{ft}, 5714\text{ft/s}, -1.3\text{deg}, 0, 15\text{deg}, 0)$$

$$(z_f, V_f) = (500\text{ft}, 335\text{ft/s})$$

$$-25 \leq \dot{z}_f \leq 8.33 \text{ (ft/s)}$$

$$(0, -\infty, 0, 0, -90\text{deg}, -90\text{deg}, -10\text{deg}, -90\text{deg}) \leq \underline{x} \leq (\infty, \infty, \infty, \infty, 90\text{deg}, 90\text{deg}, 50\text{deg}, 90\text{deg})$$

$$(-2.5g, 0, 0) \leq (n_z, \bar{q}, Q) \leq (2.5g, 700\text{lb/ft}^2, 60\text{BTU/ft}^2\text{-s})$$

The overall goal is to maximize the downrange distance, so this is implemented by minimizing the negative of the objective variable, x_f . Also, this particular formulation has an inequality control constraint limiting the AoA and AoB rates. Limits on the states are represented by the inequality “box constraints.” The infinity signs were not actually modeled as such, but made very large numbers in order to shrink the searchable region. The end-point conditions were defined for final altitude z_f , velocity v_f , and sink rate \dot{z}_f . The path constraints of normal load n_z , dynamic pressure \bar{q} , and heating rate Q , although not modeled in this “proof-of-concept”, are represented as inequality “box constraints.”

2.4 Solving the Optimal Control Problem

To demonstrate optimality, first a theoretical analysis is performed based on optimal control theory. To demonstrate the necessary conditions needed for optimality the first step requires the formulation of the Hamiltonian:

$$H(\underline{I}, x, u, t) = F(x, u, t) + \underline{I}^T f(x, u, t) \quad (12)$$

where $F(\cdot)$ is the Lagrange cost and $f(\cdot)$ is the vector field for the right hand side of the differential equations of motion. Therefore,

$$\underline{I}^T = \begin{bmatrix} I_x \\ I_y \\ I_z \\ I_v \\ I_g \\ I_x \\ I_a \\ I_s \end{bmatrix} \in \mathbb{R}^8 ; \quad \underline{x}_f = \begin{bmatrix} z_f \\ V_f \\ \dot{z}_f \end{bmatrix} \in \mathbb{R}^3 \quad (13)$$

$$\begin{aligned} H(\cdot) = & \underline{I}_x [V \cos \mathbf{g} \cos \mathbf{x}] + \underline{I}_y [V \cos \mathbf{g} \sin \mathbf{x}] + \underline{I}_z [V \sin \mathbf{g}] + \underline{I}_v \left[-\frac{1}{2m} \mathbf{r}_0 e^{-\frac{z}{z_0}} S_{ref} V^2 C_D \{\mathbf{a}\} - g \sin \mathbf{g} \right] \\ & + \underline{I}_g \left[\frac{1}{2m} \mathbf{r}_0 e^{-\frac{z}{z_0}} S_{ref} V^2 C_L \{\mathbf{a}\} - g \frac{\cos \mathbf{g}}{V} \right] + \underline{I}_y \left[\frac{\frac{1}{2} \mathbf{r}_0 e^{-\frac{z}{z_0}} S_{ref} V^2 C_L \{\mathbf{a}\} \sin \mathbf{s}}{mV \cos \mathbf{g}} \right] + \underline{I}_a u_a + \underline{I}_s u_s \end{aligned} \quad (14)$$

$$\dot{\underline{x}} = \frac{dH}{d\underline{I}} \Rightarrow \text{RHS of dynamic equations} \quad (15)$$

The Hamiltonian Minimization Condition (HMC) is based on Pontryagin's Minimum Principle such that the optimal control must minimize the Hamiltonian with respect to control. For this problem the control is subject to an inequality constraint so the Karush-Kuhn-Tucker (KKT) Theorem is applied by taking the Lagrangian of the Hamiltonian:

$$\bar{H}(\dots, u, \mathbf{m}) = H(\cdot) + \mathbf{m}^T h \quad (16)$$

where \mathbf{m} is a KKT multiplier and h is the control constraint vector. The appropriate necessary condition is:

$$\frac{\partial \bar{H}}{\partial \underline{u}} = \frac{\partial H}{\partial \underline{u}} + \left(\frac{\partial h}{\partial \underline{u}} \right)^T \mathbf{m} = 0 \quad (17)$$

and substituting (14) and the controls into (17), the HMC becomes

$$\left. \begin{array}{l} \lambda_\alpha + \mu_\alpha = 0 \\ \lambda_\phi + \mu_\phi = 0 \end{array} \right\} \Rightarrow \begin{array}{l} \lambda_\alpha = -\mu_\alpha \\ \lambda_\phi = -\mu_\phi \end{array} \quad (18)$$

Also, the multiplier-constraint pair must satisfy the following KKT Complimentarity Conditions (CC):

$$\mathbf{m}_{a,s} \begin{cases} \leq 0 & \text{if } u_{a,s} = -40 \\ = 0 & \text{if } -40 < u_{a,s} < 40 \\ \geq 0 & \text{if } u_{a,s} = 40 \end{cases} \Rightarrow u = \begin{cases} -40 & \text{if } \mathbf{m} \leq 0 \Rightarrow \mathbf{I}_{a,s} \geq 0 \\ 40 & \text{if } \mathbf{m} \geq 0 \Rightarrow \mathbf{I}_{a,s} \leq 0 \end{cases} \quad (19)$$

To determine the final value of the Hamiltonian, the Endpoint Lagrangian, given as,

$$\bar{E}(\mathbf{u}, x_f, t_f) := E(x_f, t_f) + \mathbf{u}^T e(x_f, t_f) \Rightarrow -x_f + \mathbf{u}_z(z_f - z^f) + \mathbf{u}_v(V_f - V^f) \quad (20)$$

is substituted into the Hamiltonian Value Condition (HVC):

$$H(t_f) + \frac{\partial \bar{E}}{\partial t_f} = 0 \Rightarrow H(t_f) = 0 \quad (21)$$

This indicates that the final value for the Hamiltonian should be approximately zero for this problem. Also, applying the Terminal Transversality Conditions (TTC), gives some indication of the final value of the dual variables that can be used later to confirm numerical results.

$$\underline{\mathbf{I}}(t_f) = \frac{\partial \bar{E}}{\partial \underline{x}_f} \Rightarrow \begin{bmatrix} -1 \\ 0 \\ \mathbf{u}_z \\ \mathbf{u}_v \\ 0 \\ 0 \\ 0 \\ 0 \end{bmatrix} \quad (22)$$

Likewise, the Hamiltonian Evolution Equation (HEE) is used to indicate the nature of the Hamiltonian with respect to time such that:

$$\frac{\partial H}{\partial t} = 0 \Rightarrow \frac{dH}{dt} = 0 \quad (23)$$

Here, the Hamiltonian is constant with respect to time. Combining HEE (23) with HVC (21), the Hamiltonian should be 0 for all time.

The above analysis is used throughout this study to verify that the numerical results satisfy the necessary KKT conditions for optimality. For example, the co-state values at the nodes, provided by the Covector Mapping Theorem in the Legendre Pseudospectral Method, can be substituted into the necessary conditions above to evaluate optimality.

3. Sampled-Data Feedback Control

The architecture overview for the off-line and on-line trajectory generation is shown in Fig.1 with the basic premise of the sampled-data closed-loop RV guidance and control portrayed in Figures 2 & 3.

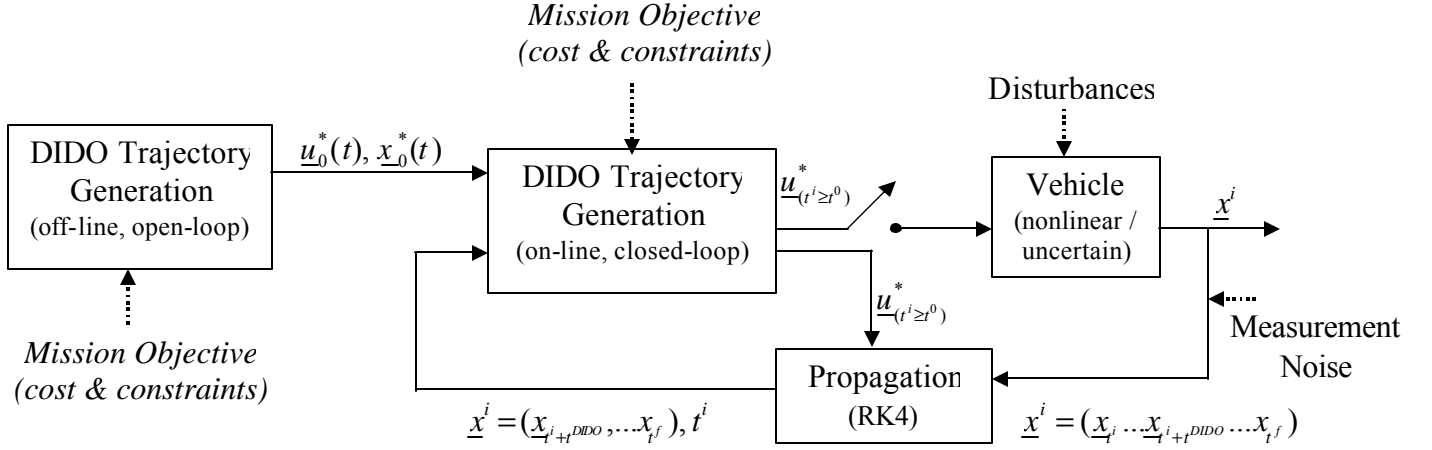


Fig. 1: Off-Line and On-Line Trajectory Generation Control Architecture

The purpose of the architecture shown in Fig.1 is to illustrate the overall systems use of an off-line optimal trajectory solution, successive on-line optimal trajectory solutions, and a simple Runge-Kutta propagation scheme to integrate the equations of motion in order to determine the current vehicle state vector. The flowchart for the actual control algorithm implemented in this work is shown in Fig.2.

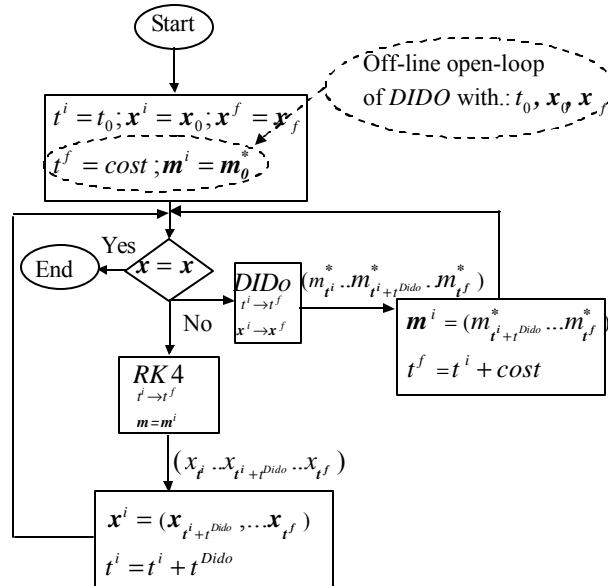


Fig 2: Closed-loop Control Algorithm [12]

The initial guidance command (i.e. the reference trajectory), is generated off-line by computing the open-loop optimal control using DIDO software to provide the initial control signal, $(\dot{\mathbf{a}}_0, \dot{\mathbf{f}}_0)$ and an estimate of the final downrange distance, x^f . The closed-loop optimal control is then solved on-line by using the off-line solution as the start-up values to a new open-loop optimal control problem with sampled data fed back from the previous DIDO run. As the next DIDO run is in progress, the equations of motion are propagated in real-time from the previously measured state vector as its initial condition using the last interpolated control vector, or if not available, the appropriate portion of the nominal control. Upon DIDO completion, the vehicle's current state is provided from the propagation routine and a new optimal trajectory is computed using the same constraints as the off-line problem. The successive re-optimization is illustrated in Fig.3 to help clarify what is happening. Not shown are the new complete optimal open-loop trajectories beginning from each successive initial condition (IC). NOTE: Propagated (RK4) segments are exaggerated for illustration purposes only.

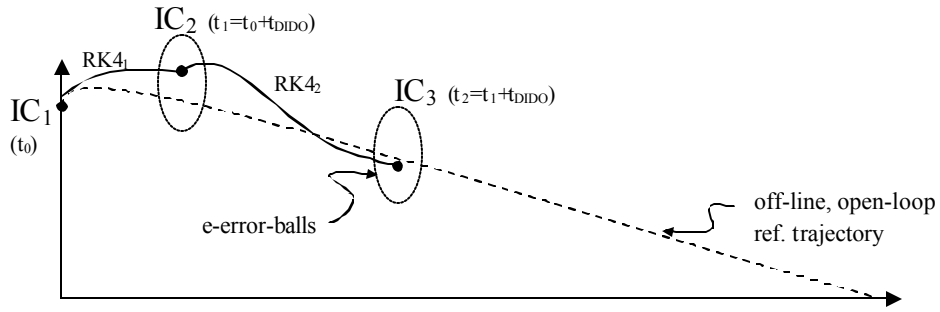


Fig. 3: Successive Re-Optimization Concept

To model external disturbances in the form of wind, wind velocity components (W_x, W_y, W_z) were augmented to the kinematical and dynamical equations of motion for the closed-loop implementation to give the following equations

$$\begin{aligned}
 \dot{x} &= V \cos \mathbf{g} \cos \mathbf{x} + W_x \\
 \dot{y} &= V \cos \mathbf{g} \sin \mathbf{x} + W_y \\
 \dot{z} &= V \sin \mathbf{g} + W_z \\
 \dot{V} &= -\frac{D\{V, z\}}{m} - g \sin \mathbf{g} - (\dot{W}_x \cos \mathbf{g} + \dot{W}_z \sin \mathbf{g}) \\
 \dot{\mathbf{g}} &= \frac{L\{V, z\}}{mV} - \frac{g \cos \mathbf{g}}{V} + \frac{1}{V} (\dot{W}_x \sin \mathbf{g} - \dot{W}_z \cos \mathbf{g}) \\
 \dot{\mathbf{x}} &= \frac{L\{V, z\} \sin \mathbf{s}}{mV \cos \mathbf{g}}
 \end{aligned} \tag{24}$$

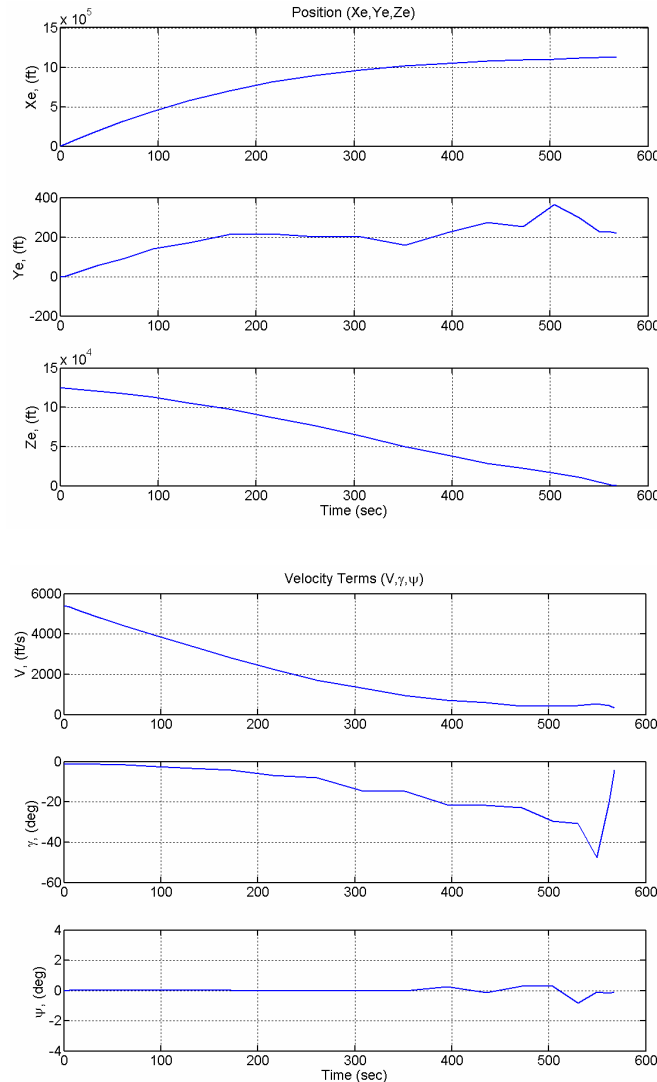
At lower altitudes, these wind velocity components typically form a wind shear that is commonly represented by a parabolic gradient as a function of altitude. For this “proof-of-concept” study, the external disturbances are kept arbitrary; hence, details of the wind gradient are not included in the model, but rather uniform, constant components are used in the equations above such that the \dot{W} terms are zero.

4. Results and Discussions

The maximum downrange trajectory of a generic RV is studied to illustrate the performance of the above on-line closed-loop control scheme.

4.1 Open-Loop Control Solution

For the reentry trajectory, the open-loop maximum-downrange solution is shown in Fig.4. It is seen that the optimal control given by the a, f -rate modulation drives the RV to a maximum downrange of approximately 1,129,593 ft (185 nm or 344 km) over a total flight time of 567 seconds and within the allowable tolerance of 6.0% for the desired end-point conditions.



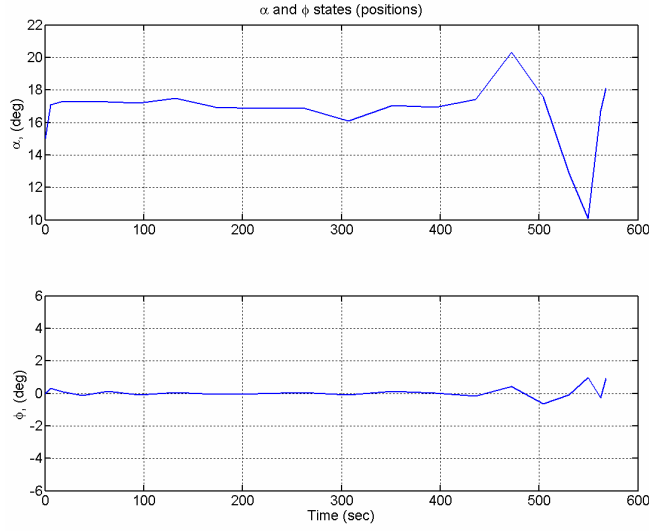


Fig. 4: Optimal Open-Loop States

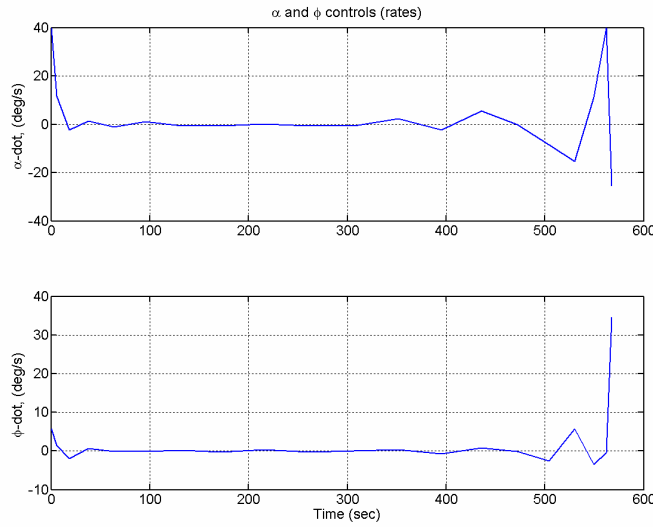


Fig. 5: Optimal Open-Loop “Virtual” Controls

For numerical optimization methods, it is always advisable to verify solution feasibility and that the necessary optimality conditions are indeed satisfied.

4.1.1 Demonstration of Computational FEASIBILITY via Propagation Comparison

The feasibility of the computational solution can be validated by comparing the DIDO results to the propagated states via a separate ODE Runge-Kutta propagator. By interpolating the values of the control function, $u(t_i)$, at the LGL points and then integrating the differential dynamical equations, $\dot{x} = f(x, u(t), t)$, via MATLAB’s ode45 solver, a comparison of error norms can be made with the DIDO trajectory results. Results showed that the open-loop system response does satisfy the end-point conditions within an acceptable error range. There is some “norm” error

between the DIDO states and the ode45-propagated states; however, this doesn't necessarily invalidate the feasibility of the computational solution. There is an obvious tradeoff between accuracy and computational execution time. According to Ref. [24], solutions using greater than 60 nodes (for a similar problem) will provide acceptable results, but at the cost of significantly more execution time. One way to improve the accuracy is to increase the number of nodes or to relax the endpoint constraint. Although this model only fixes final altitude, final velocity, and final sink rate, a real vehicle must arrive to the landing site in a controllable attitude and reasonable approach speed. As such, constraining the vehicle's final attitude could be included in the final conditions. Since the focus of this paper is to demonstrate successful implementation of the optimal closed-loop feedback, the fastest execution time possible is sought within acceptable error tolerances. For more on DIDO performance for this type of problem, refer to Ref.[24].

4.1.2 Demonstration of Computational OPTIMALITY via Bellman's Principle

Comparing the numerical results to the above theoretical analysis of the HVC, HEE, HMC, and TTC conditions validates the optimality of the computational solution. The HVC stated in the theoretical analysis indicates that the Hamiltonian should be 0 at the final time (i.e. $H(t_f)=0$). From the HEE, it can be shown that the Hamiltonian is constant with respect to time. Combining these two conditions, the Hamiltonian should be 0 for all time, clearly evident in Fig.6. Likewise, the Lagrange multipliers for the dynamics at the final time match the theoretical TTC results (not shown).

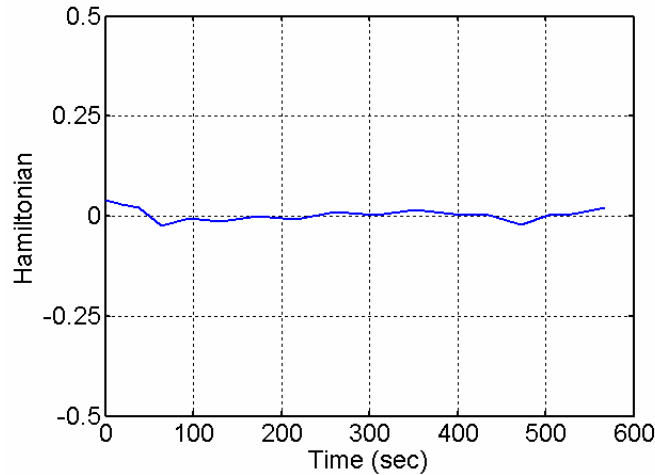


Fig. 6: Hamiltonian from Open-Loop Solution

Another test to confirm computational optimality is to apply Bellman's Principle of Optimality. This principle essentially states that by using any point on the original optimal trajectory as an initial condition to a new problem (with all other problem formulation parameters the same) should result in the same optimal trajectory with the same or better cost. Although it is not shown here, this method was used to validate optimality.

4.4 Closed-Loop Control Solution

Although the previous open-loop solution results in a feasible trajectory and desired end-point conditions that satisfy the necessary conditions for optimality, it does not account for any external disturbances as would be the case in real applications. Well known is that without some form of feedback, disturbances, in the form of parameter uncertainty, sensor measurement errors (e.g. noise), or unknown/unpredictable external forces/moments, can result in significantly degraded system performance. To illustrate the effects of external disturbances for this reentry problem, a simulated wind gust was applied over a period of 20 sec beginning at 200 sec into the flight. Sensor measurement errors and parameter uncertainty can be simulated by assuming the role of the errors from the numerical propagation. The effects of the wind on the open-loop (OL) trajectory are seen in Fig. 7. Fig. 8 shows the closed-loop (CL) results for the variables of interest.

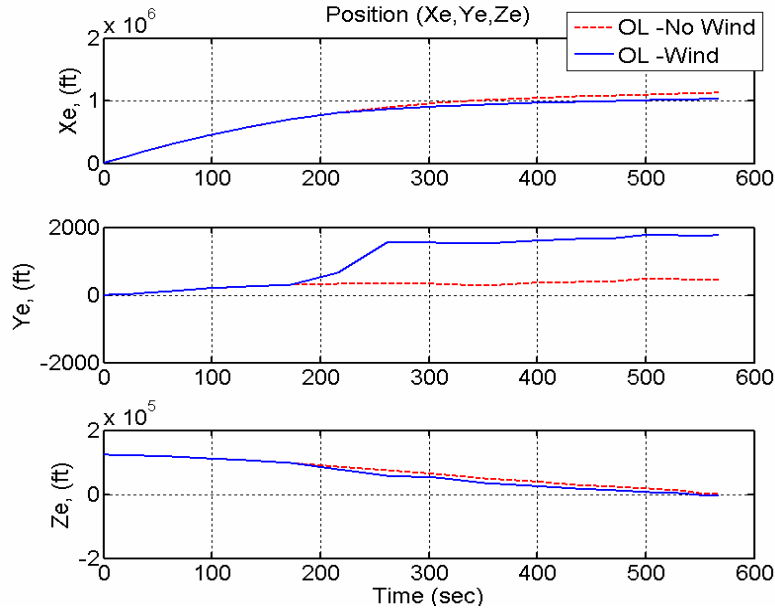


Fig. 7: Open-Loop (OL) System Response with “Nominal” Wind Gust

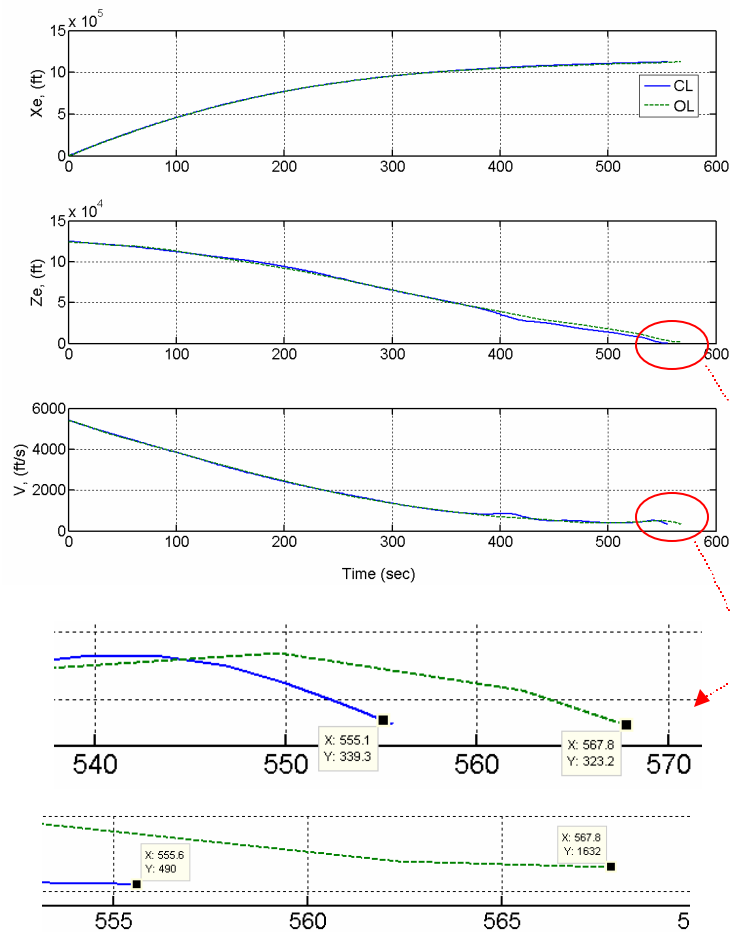


Fig. 8: System Response with “Nominal” Wind Gust

To further illustrate how the closed-loop system can recover from the effects of an external disturbance, Fig.10 compares the results of an exaggerated 600 ft/sec (~355 knot) downburst of wind, often referred to as a “microburst,” applied over a 60 second period. It is evident from figures 11 and 12 that the open-loop system cannot recover from the microburst. The vehicle is slammed into the ground for the open-loop trajectory (-5207 ft), where as the closed-loop trajectory corrects for the microburst and is able to achieve a final altitude of 490 ft, within 10 ft of the desired final altitude and within the allowable end-point tolerance.

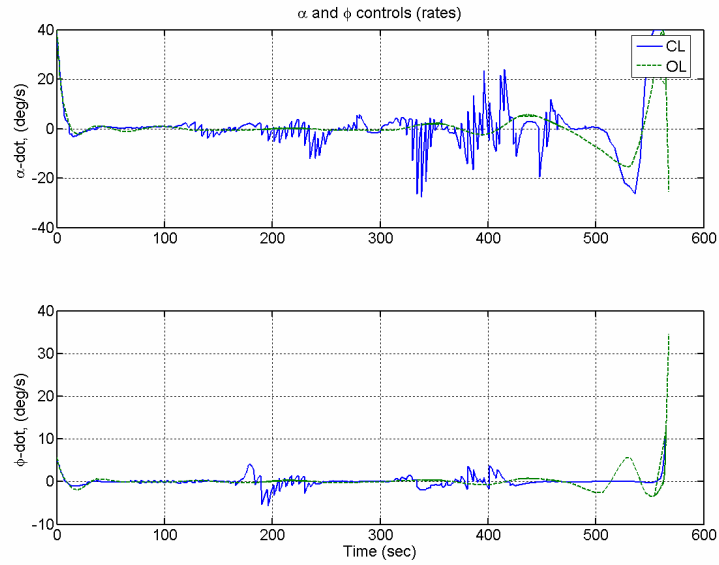


Fig. 9: System Controls for “Nominal” Wind Gust

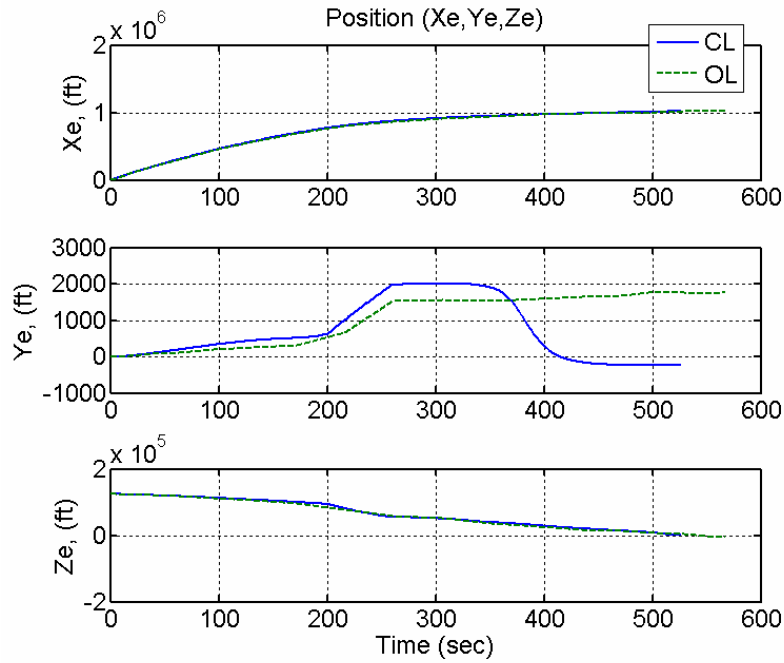


Fig. 10: System Response to “Exaggerated” Wind Gust

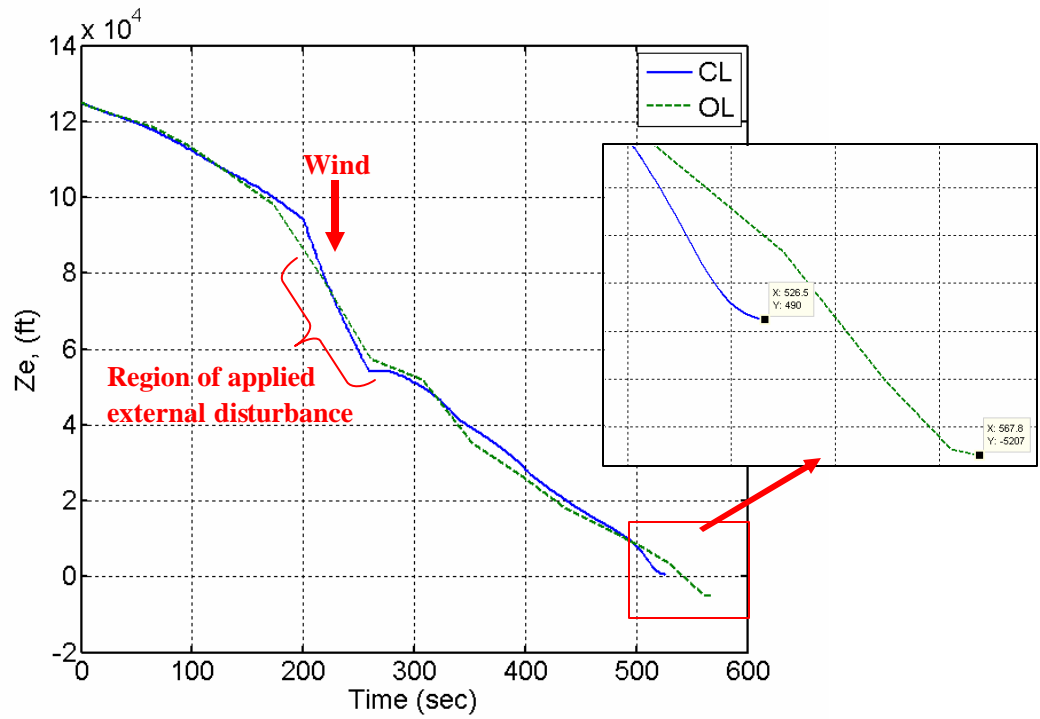


Fig. 11: Effects on Altitude with "Exaggerated" Wind Gust

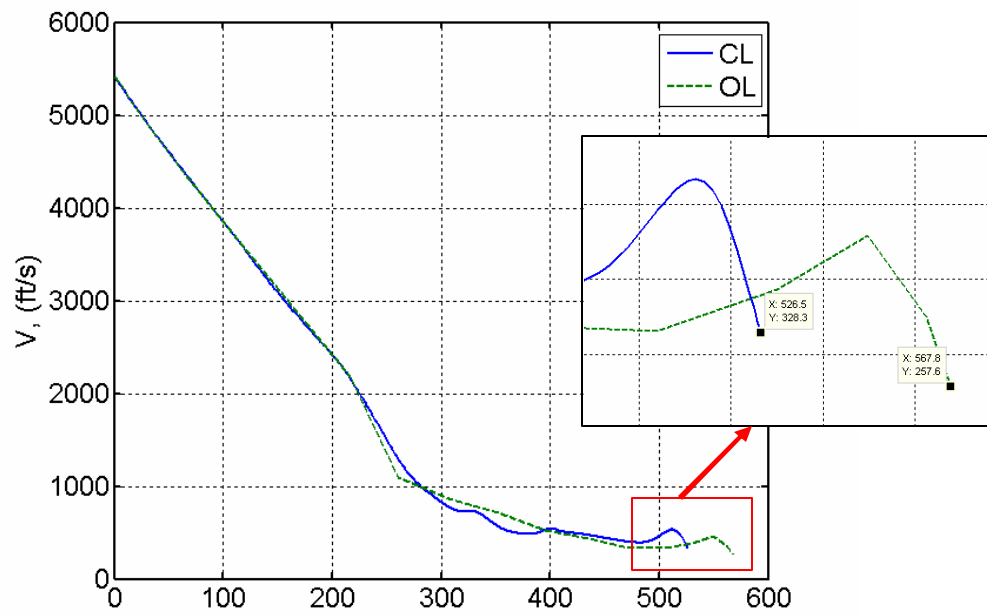


Fig. 12: Effects on Velocity with "Exaggerated" Wind Gust

Success of this feedback method depends on relatively fast re-computation time. Computation of the first off-line, open-loop optimal control trajectory takes 11 seconds and the subsequent open-loop optimal control updates are computed within 0.60 to 11.5 seconds. The feedback computation times are shown over the entire trajectory in Fig.13. These trajectories were generated on a Dell Optiplex Desktop with a Pentium M, 3.40 Ghz processor, and 1.0 GB of RAM.

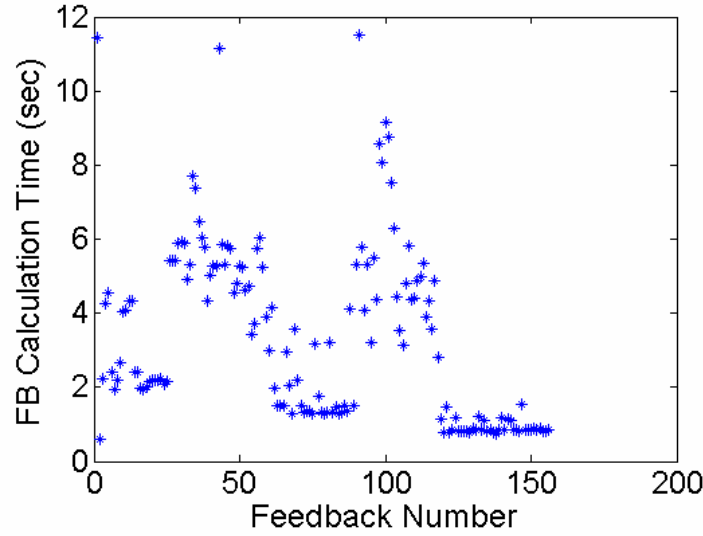


Fig. 13: Feedback Computation Times for System with “Nominal” Disturbance

For this problem, there were no error-balls (ϵ) around the initial conditions for each successive update problem as Pooya used in the time-optimal satellite slew maneuver problem [12]. This means that it is more likely that the re-optimized closed-loop trajectories will not follow the original, off-line open-loop response. According to Bellman’s Principle, without the presence of disturbances, the re-optimized closed-loop trajectory should follow the original optimal open-loop trajectory. By allowing an epsilon-error ball around the initial conditions, there should be less distinction between the old and new trajectories; hence, the new trajectory is literally a “neighboring” extremal. When disturbances are present, the optimal trajectory changes with each re-optimization step and are feedback to the system. This results in a different control trajectory as seen in Fig.14. This unique control history applied to the system with external disturbances is capable of countering their effects and driving the vehicle to the desired end point conditions, primarily altitude and velocity in this problem.

A potential drawback for this approach has to do with the fact that the optimal controls, at each successive re-optimization step, can essentially be reset to some drastically different value within the control constraint bounds as opposed to the states that must start at the previous position vector. This “jump” in the controls is illustrated in Fig.14 and can be resolved by placing a similar tolerance or ϵ -error-ball on the initial control vector for each re-optimization problem, such as $|\underline{u}(0)_{k+1} - \underline{u}_k| < \epsilon$, where ϵ is some predefined tolerance.

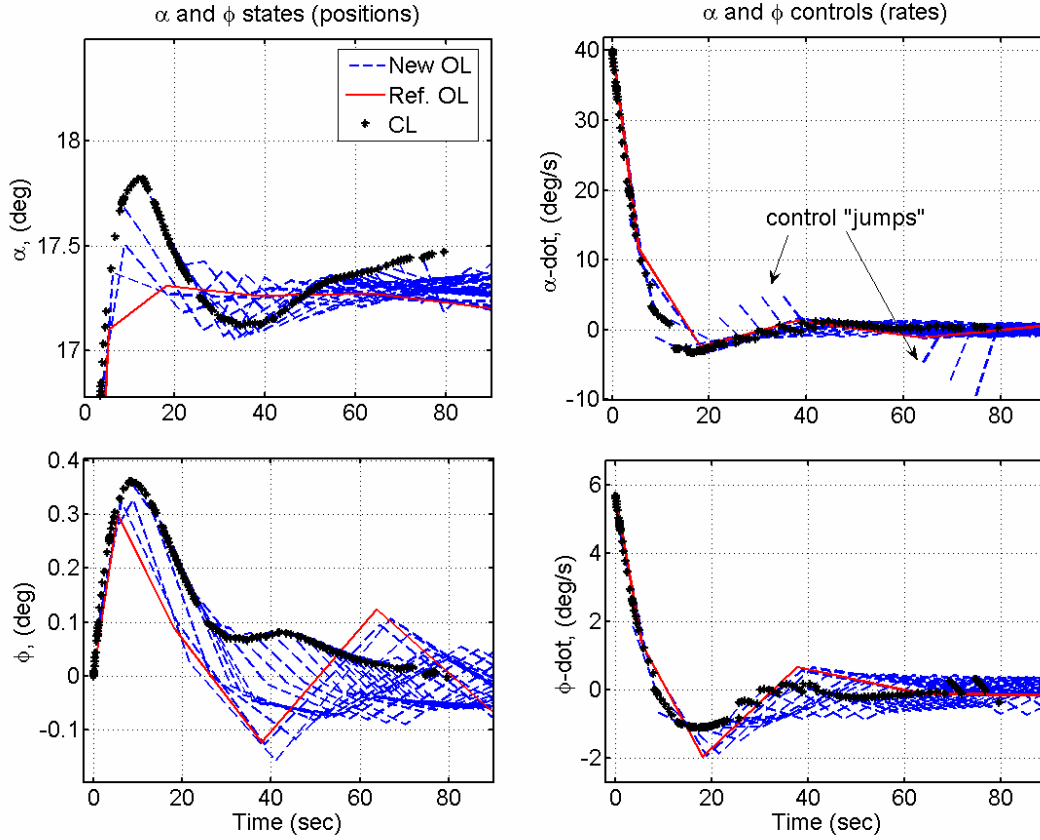


Fig. 14: Example of Successive Re-Optimization with Control “Jumps”

Another potential problem is that of convergence. If for some reason, one of the re-optimization steps does not converge, it can crash the entire closed-loop process; however, additional logic can be built into the feedback algorithm to prevent the convergence issue from crashing the system. Such logic, as previously mentioned, may include using the previous “good” solution for some finite time and then attempting a new re-optimization. In the event of frequent or repetitive non-convergence issues, the only option may be to revert back to using the open-loop response for the remaining trajectory. Of course this would only be practical if the remaining time-to-go is relatively short and there are minimum uncertainties and/or disturbances during this time. If not, at least a “hard” crash is prevented and the possibility of a feasible trajectory still exists.

5. Conclusions

In this paper, a sampled-data feedback control law, constructed from successive optimal open-loop solutions, was used to generate online, optimal trajectories for the reentry of a generic reusable launch vehicle. It was shown that rapid re-computation of the open-loop optimal control can effectively be used for online trajectory generation in the presence of various disturbances and uncertainties. A significant advantage of this control scheme is that it does not require any advance knowledge of feedback computation times; hence, no prediction method is

required. As demonstrated, solutions to difficult problems that may require feedback such as on-line trajectory generation in the face of disturbances are now possible.

Acknowledgment

The authors would like to extend their appreciation to Dr. Pooya Sekhavat, visiting post-doc research assistant at the Guidance, Navigation, and Control (GNC) Laboratory, Naval Postgraduate School, for his help with implementing and debugging the sampled-data feedback algorithm. His efforts are greatly appreciated.

References

1. Harpold, J.C., and Graves, C.A., "Shuttle Entry Guidance," *The Journal of Astronautical Sciences*, Vol. 27, No. 3, pp.239-268, Jul-Sep 1979.
2. Oppenheimer, M.W., and Doman, D.B., "Reconfigurable Control Design for the X-40A with In-Flight Simulation Results," *Proceedings of the 2005 AIAA Guidance, Navigation, and Control Conference*, AIAA Paper No. 2004-5017, Aug 2004.
3. Oppenheimer, M.W., and Doman, D.B., "Reconfigurable Inner Loop Control of a Space Maneuvering Vehicle," *Proceedings of the 2003 AIAA Guidance, Navigation, and Control Conference*, AIAA Paper No. 2003-5358, Aug 2003.
4. Bolender, M.A., and Doman, D.B., "Nonlinear Control Allocation Using Piecewise Linear Functions," *Journal of Guidance, Control, and Dynamics*, Vol.27, No. 6, pp.1017-1027, 2004.
5. Doman, D.B., and Oppenheimer, M.W., "Integrated Adaptive Guidance and Control for Space Access Vehicles, Volume 1: Reconfigurable Control Law for X-40A Approach and Landing," *AFRL IAG&C Technical Report*, Wright-Patterson AFB, OH, 2004.
6. Schierman, J.D., Hull, J.R., and Ward, D.G., "On-Line Trajectory Command Reshaping for Reusable Launch Vehicles," *Proceedings of the 2003 AIAA Guidance, Navigation, and Control Conference*, AIAA Paper No. 2003-5439, Aug 2003.
7. Schierman, J.D., Hull, J.R., and Ward, D.G., "Adaptive Guidance with Trajectory Reshaping for Reusable Launch Vehicles," *Proceedings of the 2002 AIAA Guidance, Navigation, and Control Conference*, AIAA Paper No. 2002-4458, Aug 2002.
8. Shaffer, P.J., Ross, I.M., Oppenheimer, M.W., Doman, D.B., "Optimal Trajectory Reconfiguration and Retargeting for a Reusable Launch Vehicle," *Proceedings of the 2005 AIAA Guidance, Navigation, and Control Conference*, AIAA Paper No. 2005-4168, Aug 2005.
9. Schierman, J.D., Hull, J.R., "In-Flight Entry Trajectory Optimization for Reusable Launch Vehicles," *Proceedings of the 2005 AIAA Guidance, Navigation, and Control Conference*, AIAA Paper No. 2005-6434, Aug 2005.
10. Carson, J.M., Epstein, M.S., MacMynowski, D.G., and Murray, R.M., "Optimal Nonlinear Guidance With Inner-Loop Feedback for Hypersonic Re-Entry," Paper submitted to *American Control Conference*, 2005.
11. Milam, M.B., Mushambi, K., and Murray, R.M., "A New Computational Approach to Real-Time Trajectory Generation for Constrained Mechanical Systems," *Conference on Decision and Control*, 2000.
12. Pooya, S., Fleming, A., and Ross, I.M., "Time-Optimal Nonlinear Feedback Control for the NPSAT 1 Spacecraft," *Proceedings of the 2005 IEEE/ASME*, Jul 2005.
13. Schierman, J.D., Ward, D.G., Monaco, J.F., and Hull, J.R., "Reconfigurable Guidance Approach for Reusable Launch Vehicles," *Proceedings of the 2001 AIAA Guidance, Navigation, and Control Conference*, AIAA Paper No. 2001-4429, Aug 2001.
14. Pesch, H.J., "Off-Line and On-Line Computation of Optimal Trajectories in the Aerospace Field," Prepared for the 12th Course in *Applied Mathematics in the Aerospace Field* of the International School of Mathematics, Ettore Majorana Centre for Scientific Culture, Sicily, Sept 1991.
15. Ross, I.M., and Fahroo, F., "Legendre Pseudospectral Approximations of Optimal Control Problems," *Lecture Notes in Control and Information Sciences*, Vol. 295, Springer-Verlag, New York, pp.327-342, 2003.

16. Ross, I.M., and Fahroo, F., "Issues in the Real-Time Computation of Optimal Control," *Mathematical and Computer Modeling*, An International Journal, Vol. 40, Pergamon Publication, to appear.
17. Ross, I.M., and Fahroo, F., "Pseudospectral Knotting Methods for Solving Optimal Control Problems," *Journal of Guidance, Control, and Dynamics*, Vol. 27, No. 3, pp.397-405, 2004.
18. Ross, I.M., Fahroo, F., and Gong, Q., "A Spectral Algorithm for Pseudospectral Methods in Optimal Control," *Proceedings of the 6th IASTED International Conference on Intelligent Systems and Control*, Honolulu, HI, 2004.
19. Ross, I.M., and Fahroo, F., "User's Manual for DIDO 2002: A MATLAB Application Package for Dynamic Optimization," NPS Technical Report AA-02-002, Department of Aeronautics and Astronautics, Naval Postgraduate School, Monterey, CA, June 2002.
20. Josselyn, S. and Ross, I.M., "Rapid Verification Method for the Trajectory Optimization of Reentry Vehicles," *Journal of Guidance, Control, and Dynamics*, Vol.26, No. 3, pp.505-508, 2002.
21. Strizzi, J., Ross, I.M., and Fahroo, F., "Towards Real-Time Computation of Optimal Controls for Nonlinear Systems," *Proceedings of the 2002 AIAA Guidance, Navigation, and Control Conference*, AIAA Paper No. 2002-4945, Aug 2002.
22. Regan, F.J., and Anandakrishnan, S.M., *Dynamics of Atmospheric Re-Entry*, AIAA Education Series, Washington D.C., 1993.
23. Betts, J.T., *Practical Methods for Optimal Control Using Nonlinear Programming*, Society for Industrial and Applied Mechanics (SIAM), Philadelphia, PA 2001.
24. Shaffer, Patrick J., *Optimal Trajectory Reconfiguration and Retargeting for the X-33 Reusable Launch Vehicle*, Thesis, Naval Postgraduate School, Monterey, CA, 2004.